IOP Publishing | Astro Ltd Laser Physics

Laser Phys. **25** (2015) 035402 (7pp) doi:10.1088/1054-660X/25/3/035402

Energy transfer between two filaments and degenerate four-photon parametric processes

Daniela A Georgieva[1] **and Lubomir M Kovachev**[2]

[1] Faculty of Applied Mathematics and Computer Science, Technical University of Sofia, 8 Kliment Ohridski Blvd., 1000 Sofia, Bulgaria
[2] Institute of Electronics, Bulgarian Academy of Sciences, Tzarigradcko shossee 72, 1784 Sofia, Bulgaria

E-mail: lubomirkovach@yahoo.com

Received 25 September 2014, revised 24 December 2014
Accepted for publication 3 January 2015
Published 4 February 2015

Abstract

Recently, energy exchange between two filaments crossing at small angle and with power slightly above the critical for self-focusing P_{cr} was experimentally demonstrated. In this paper we present a model describing the process of this transfer through degenerate four-photon parametric mixing. Our model confirms the experimental results that the direction of energy exchange depends on the relative transverse velocity (incident angle), laser intensity and initial distance between the pulses (relative initial phase). We also investigate the interaction between two collinear filaments in order to explain the filament number reduction for powers close to P_{cr} in multi-filamental propagation.

Keywords: dynamics of nonlinear optical systems, optical instabilities, optical chaos and complexity, optical spatio-temporal dynamics

(Some figures may appear in colour only in the online journal)

1. Introduction

Several experimental works [1–3] report intensive exchange of energy when two filaments with the same carrying frequency intersect at a small angle. The mechanisms for energy exchange proposed in [1, 2] require two different main frequencies of the pulses. The experiment described in [3] is performed at a single pulse frequency. The authors of [3] add another mechanism as a possible explanation—nonlinear absorption at high input power. All experiments were performed with filament power slightly above the critical value for self-focusing P_{cr}. This is the reason to look for other mechanisms leading to exchange of energy and connected with nonlinear optical effects. To do that, we take into account the following experimental details. First, the laser pulses propagating on different optical trajectories always intersect with a relative phase difference. This means that at the intersection region there are conditions for degenerate four-photon parametric (FPP) processes. As is mentioned in [4], the degenerate FPP processes play an important role also in the multi-component filamentation generation. Another important experimental observation in the multi-filament propagation is the significant reduction in the number of filaments as a function of the distance [5–7].

In this manuscript we propose a nonlinear vector model including degenerate FPP process. We investigate numerically the interaction between optical pulses during their propagation in air for the cases when (1) the components of the polarization vector are separated, (2) the filaments contain the two polarization components (the polarization components are not separated, general case). The phenomenon of the reduction of the number of filaments in a multi-filament propagation is also studied in our model. We found that at least two different nonlinear physical mechanisms lead to reduction of the number of filaments. In this paper we will analyse one of them: decreasing of the number of filaments due to energy exchange in one degenerate FPP mixing process. The numerical scheme is performed on the basis of the split-step Fourier method.

2. Nonlinear polarization

As demonstrated in [8], high intensity femtosecond pulses generate in gases stable filaments with a broad-band spectrum.

Various models explaining this phenomenon are presented (see for example the paper of Couairon and Mysyrowicz and references therein [6]). The standard filamentation model is based on plasma generation and multi-photon processes and includes also nonlinear polarization of the kind

$$\vec{P}^{\,\mathrm{nl}} = n_2\left[\left(\vec{E}\cdot\vec{E}^{*}\right)\vec{E} + \frac{1}{2}\left(\vec{E}\cdot\vec{E}\right)\vec{E}^{*}\right], \tag{1}$$

where n_2 is the nonlinear refractive index of the isotropic media. The polarization (1) was proposed by Maker and Terhune in 1965 [9]. If the electrical field contains one linear or circular component, the polarization (1) describes only the self-action effect, while in the case of two-component electrical filed $\vec{E} = \left(E_x, E_y, 0\right)$ additional terms appear, presenting cross-modulation and degenerate four-photon parametric mixing. The self-action process broadens the pulse spectrum—starting from narrow-band pulse, the stable filament becomes broad-band far way from the source. Later [10–12] show, though, that the evolution of broad-band pulses like filaments can not be described correctly by nonlinear polarization of the kind (1). It is more correct to use the generalized vector nonlinear operator [13]

$$\vec{P}^{\,\mathrm{nl}} = n_2\left(\vec{E}\cdot\vec{E}\right)\vec{E}, \tag{2}$$

which includes additional processes associated with third harmonic generation (THG). One precise analysis, presented in the present paper, demonstrates that the polarization of kind (2) is not applicable to a scalar model, because the corresponding Manley–Rowe (MR) conservation laws are not satisfied. That is why we substitute into the nonlinear operators (1) and (2) a two-component electrical vector field at one carrying frequency of the form:

$$\vec{E} = \frac{\left(A_x \exp\left(\mathrm{i}\omega_0 t\right) + \mathrm{c.c.}\right)}{2}\vec{x} + \frac{\left(A_y \exp\left(\mathrm{i}\omega_0 t\right) + \mathrm{c.c.}\right)}{2}\vec{y}, \tag{3}$$

where $A_x = A_x(x, y, z, t)$, $A_y = A_y(x, y, z, t)$ are the amplitude functions and ω_0 is the carrying frequency of the laser source.

In the case of Maker and Terhune polarization (1) we obtain

$$\begin{aligned}
\vec{P}_x^{\,\mathrm{nl}} &= \frac{3}{8}n_2\left[\left(|A_x|^2 + \frac{2}{3}|A_y|^2\right)A_x + \frac{1}{3}A_x^{*}A_y^{2}\right]\exp\left(\mathrm{i}\omega_0 t\right) + \mathrm{c.c.}\\
\vec{P}_y^{\,\mathrm{nl}} &= \frac{3}{8}n_2\left[\left(|A_y|^2 + \frac{2}{3}|A_x|^2\right)A_y + \frac{1}{3}A_y^{*}A_x^{2}\right]\exp\left(\mathrm{i}\omega_0 t\right) + \mathrm{c.c.}
\end{aligned} \tag{4}$$

The nonrestricted nonlinear polarization (2) generates the following components

$$\begin{aligned}
\vec{P}_x^{\,\mathrm{nl}} &= \tilde{n}_2\left[\tfrac{1}{3}\left(A_x^2 + A_y^2\right)A_x\exp(2\mathrm{i}\omega_0 t)\right.\\
&\quad\left.+\left(|A_x|^2 + \tfrac{2}{3}|A_y|^2\right)A_x + \tfrac{1}{3}A_x^{*}A_y^{2}\right]\exp(\mathrm{i}\omega_0 t) + \mathrm{c.c.}\\
\vec{P}_y^{\,\mathrm{nl}} &= \tilde{n}_2\left[\tfrac{1}{3}\left(A_x^2 + A_y^2\right)A_y\exp(2\mathrm{i}\omega_0 t)\right.\\
&\quad\left.+\left(|A_y|^2 + \tfrac{2}{3}|A_x|^2\right)A_y + \tfrac{1}{3}A_y^{*}A_x^{2}\right]\exp(\mathrm{i}\omega_0 t) + \mathrm{c.c.},
\end{aligned} \tag{5}$$

where $\tilde{n}_2 = 3/8\, n_2$. Comparing (4) and (5), it is clearly seen that the operator (2) $n_2\left(\vec{E}\cdot\vec{E}\right)\vec{E}$ generalizes the case of Marker and Terhune's operator (1), but includes also additional terms associated with THG.

3. Basic system of equations

The stable filament propagation in gases is realized in the sub-pico and femtosecond regions, while in the nano- and picosecond regions appears the well known self-focusing. The dynamics of narrow-band laser pulses can be accurately described in the frame of paraxial optics. The filamentation experiments demonstrate a typical pulse spectrum evolution. The initial laser pulse ($t_0 \geqslant 50$ fs) possesses a relatively narrow-band spectrum ($\Delta k_z \ll k_0$), where Δk_z is the spectral pulse width and k_0 is the carrying wave number. During the filamentation process the initial self-focusing broadens significantly the pulse spectrum. The broad-band spectrum is one of the basic characteristics of the stable filament. The evolution of the so obtained filament can not be further described in the frame of the nonlinear paraxial optics because the paraxial optics works correctly for narrow-band laser pulses only. The dynamics of broad-band pulses can be presented properly within different non-paraxial models such as UPPE [10, 11] or non-paraxial envelope equations [12, 14]. Another standard restriction in the filamentation theory is the use of one-component scalar approximation of the electrical field $\vec{E}$. This approximation though, is in contradiction with recent experimental results, where rotation of the polarization vector is observed [15]. For this reason, in the present paper we use the non-paraxial vector model up to second order of dispersion, in which the nonlinear effects are described by the nonlinear polarization components (5). The system of non-paraxial equations of the amplitude functions A_x, A_y of the two-component electrical field (3) has the form

$$\begin{aligned}
&-2\mathrm{i}\frac{k_0}{v_{\mathrm{gr}}}\frac{\partial A_x}{\partial t} = \Delta_{\perp}A_x - \frac{\beta+1}{v_{\mathrm{gr}}}\left(\frac{\partial^2 A_x}{\partial t^2} - 2v_{\mathrm{gr}}\frac{\partial^2 A_x}{\partial t\partial z}\right)\\
&-\beta\frac{\partial^2 A_x}{\partial z^2} + k_0^2\tilde{n}_2\left[\frac{1}{3}\left(A_x^2 + A_y^2\right)A_x\right.\\
&\exp\left(2\mathrm{i}k_0\left(z - \left(v_{\mathrm{ph}} - v_{\mathrm{gr}}\right)t\right)\right) + \left(|A_x|^2 + \frac{2}{3}|A_y|^2\right)A_x\\
&\qquad\left.+\frac{1}{3}A_x^{*}A_y^{2}\right]\\
&-2i\frac{k_0}{v_{\mathrm{gr}}}\frac{\partial A_y}{\partial t} = \Delta_{\perp}A_y - \frac{\beta+1}{v_{\mathrm{gr}}}\left(\frac{\partial^2 A_y}{\partial t^2} - 2v_{\mathrm{gr}}\frac{\partial^2 A_y}{\partial t\partial z}\right)\\
&-\beta\frac{\partial^2 A_y}{\partial z^2} + k_0^2\tilde{n}_2\left[\frac{1}{3}\left(A_x^2 + A_y^2\right)A_y\right.\\
&\exp\left(2\mathrm{i}k_0\left(z - \left(v_{\mathrm{ph}} - v_{\mathrm{gr}}\right)t\right)\right) + \left(|A_y|^2 + \frac{2}{3}|A_x|^2\right)A_y\\
&\qquad\left.+\frac{1}{3}A_y^{*}A_x^{2}\right],
\end{aligned} \tag{6}$$

where $\tilde{n}_2 = 3/8\ n_2$, v_{gr} and v_{ph} are the group and phase velocities correspondingly, $\beta = k_0 v_{gr}^2 k''$ and k'' is the group velocity dispersion.

This model describes the ionization-free filamentation regime, where the pulse intensities are close to the critical one for self-focusing. The first nonlinear term in (6) corresponds to coherent GHz generation [12]. The system (6) is written in Galilean frame ($z' = z - vt$; $t' = t$) and not in the standard local time frame ($t' = t - z/v$; $z' = z$). In all coordinate systems—laboratory, moving in time, and Galilean, the group velocity adds an additional phase (carrier-envelope phase) in the third harmonic terms and transforms them to GHz ones. This can be seen directly for the system (6) written in Galilean frame, which determines the choice of coordinates. The last nonlinear term in (6) describes degenerate four-photon parametric mixing (FPM).

The system of equations (6) written in dimensionless form becomes

$$
\begin{aligned}
&-2\mathrm{i}\alpha\delta^2\frac{\partial A_x}{\partial t} = \Delta_\perp A_x - \delta^2(\beta+1)\left(\frac{\partial^2 A_x}{\partial t^2} - \frac{\partial^2 A_x}{\partial t\partial z}\right) - \delta^2\beta\frac{\partial^2 A_x}{\partial z^2}\\
&+\gamma\left[\frac{1}{3}\left(A_x^2 + A_y^2\right)A_x \exp\left(2\,\mathrm{i}(\alpha z - \widetilde{\omega}_{\mathrm{nl}} t)\right) + \left(|A_x|^2 + \frac{2}{3}|A_y|^2\right)A_x\right.\\
&\left.\quad + \frac{1}{3}A_x^* A_y^2\right]\\
&-2\mathrm{i}\alpha\delta^2\frac{\partial A_y}{\partial t} = \Delta_\perp A_y - \delta^2(\beta+1)\left(\frac{\partial^2 A_y}{\partial t^2} - \frac{\partial^2 A_y}{\partial t\partial z}\right) - \delta^2\beta\frac{\partial^2 A_y}{\partial z^2}\\
&+\gamma\left[\frac{1}{3}\left(A_x^2 + A_y^2\right)A_y \exp\left(2\,\mathrm{i}(\alpha z - \widetilde{\omega}_{\mathrm{nl}} t)\right) + \left(|A_y|^2 + \frac{2}{3}|A_x|^2\right)A_y\right.\\
&\left.\quad + \frac{1}{3}A_y^* A_x^2\right], \qquad (7)
\end{aligned}
$$

where $x = x/r_0$, $y = y/r_0$, $z = z/z_0$, $t = t/t_0$ are the dimensionless coordinates, r_0 is the pulse waist, $z_0 = v_{gr}t_0$ is the spatial pulse length, $\alpha = k_0 z_0$, $\delta = r_0/z_0$, $\gamma = k^2{}_0 r^2{}_0 \tilde{n}_2 |A_0|^2/2$ is the nonlinear coefficient and $\widetilde{\omega}_{\mathrm{nl}} = k_0\left(z - (v_{ph} - v_{gr})\right)t_0$ is the normalized nonlinear frequency.

4. Conservation laws

The nonlinear theories based on the polarization of Maker and Terhun type (1) satisfy the MR relations. This means that during the process of energy exchange the total energy is conserved for arbitrary localized smooth complex fields. Additional conservation quantities are also possible. To satisfy the MR relations of the truncated equations with a generalized nonlinear polarization of type $\vec{P}^{\mathrm{nl}} = n_2\left(\vec{E}\cdot\vec{E}\right)\vec{E}$, some restrictions on the components of the electrical field are imposed. We will demonstrate this on the basis of the two-component vector field $\vec{E} = \left(A_x, A_y, 0\right)\exp\left[\mathrm{i}k_0(z - v_{ph}t)\right]$. Let us rewrite the generalized nonlinear polarization (2) using circularly polarized components [4, 16]

$$A_+ = \left(A_x + \mathrm{i}A_y\right)/\sqrt{2}, A_- = \left(A_x - \mathrm{i}A_y\right)/\sqrt{2}\,. \qquad (8)$$

Thus we obtain

$$P_+ = n_2\left(A_+^2 A_-\right)\exp\left[\mathrm{i}k_0(z - v_{ph}t)\right] \qquad (9)$$

$$P_- = n_2\left(A_-^2 A_+\right)\exp\left[\mathrm{i}k_0(z - v_{ph}t)\right], \qquad (10)$$

where by convention P_+ and P_- correspond to left-hand circular and to right-hand circular polarization. The truncated equations can be written as

$$\mathrm{i}\frac{\partial A_+}{\partial t} = n_2\left(A_+^2 A_-\right) \qquad (11)$$

$$\mathrm{i}\frac{\partial A_-}{\partial t} = n_2\left(A_-^2 A_+\right). \qquad (12)$$

The equations for the square modulus of the components A_+ and A_- are

$$\mathrm{i}\frac{\partial |A_+|^2}{\partial t} = n_2|A_+|^2\left(A_+A_- - A_+^* A_-^*\right) = 0 \qquad (13)$$

$$\mathrm{i}\frac{\partial |A_-|^2}{\partial t} = n_2|A_-|^2\left(A_+A_- - A_+^* A_-^*\right) = 0,$$

following from the fact that the components A_+ and A_- are complex-conjugated fields (8). Thus we prove that to satisfy the MR conditions for the nonlinear system (7) (or other conservative nonlinear equations) with nonlinear operator of kind (2), the possible initial conditions and solutions should be complex-conjugated fields. The conservation laws (13) give us additional information on the behavior of the vector amplitude function: only components of the vector amplitude field $\vec{A} = \left(A_x, A_y, 0\right)$, which present rotation of the vector $\vec{A}$ in the plane (x, y), satisfy the MR conditions. That is why in our numerical experiments, as well as in our analytical investigations, we will use complex-conjugated components only.

5. Numerical simulations and discussions

We investigate numerically the following two basic nonlinear effects in the filamentation process—the energy exchange between two non-collinear filaments and the phenomenon of reducing the number of filaments in multi-filamentation propagation. We demonstrate that both processes are based on degenerate FPP mixing. The numerical simulations are carried out by using the split-step Fourier method. All our calculation are performed for propagation of fs laser pulses at main wavelength 800 nm in air. The numerical results are presented for initial conditions: 240 fs Gaussian bullet with waist and spatial length $r_0 = z_0 = 72\ \mu$m and power slightly above P_{cr}. In this case $\alpha = 200\pi$, $\delta = 1$, $\widetilde{\omega}_{\mathrm{nl}} = 0.00023$ and $\gamma \in 1.5$–3. The phase difference between the two components is initially $\pi/2$ in order to satisfy the conservation laws.

5.1. Energy exchange between two non-collinear filaments

Let us begin our consideration with the case when two laser pulses with the same carrying frequency intersect at a small angle. The pulse power is slightly above the critical for self-focusing P_{cr}.

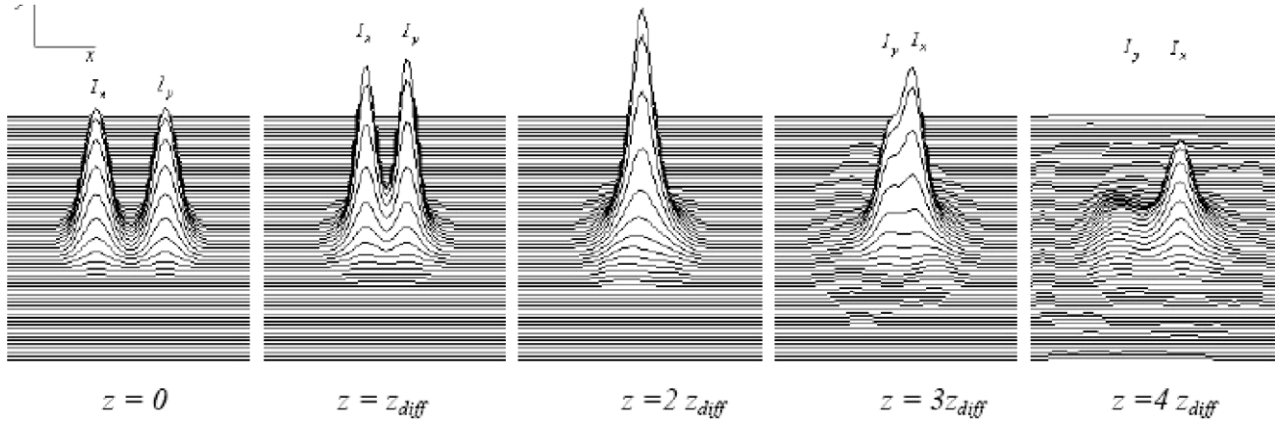

Figure 1. Collision dynamics between two separated polarization components at initial distance $2a = 4$, transverse velocity difference $2\Delta v = 0.4$, and nonlinear coefficient $\gamma = 1.8$, governed by the system of equations (7) with initial conditions (14). In the process of collision we observe self-focusing and periodic exchange of energy. The initial energy transfer is from $I_x = I_1$ to $I_y = I_2$. With z_{diff} is denoted the diffraction lengths $z_{\mathrm{diff}} = k_0 r_0^2$. The (x, y)–(spot) projection of the pulses intensities $I_{x,\,y}(x, y, z = Nz_{\mathrm{diff}}, t = Nz_{\mathrm{diff}}/v_{\mathrm{gr}})$ at distances $z = N^* z_{\mathrm{diff}}$ where $N = 0, 1..4$. The same kind of spot projections are plotted in the following figures.

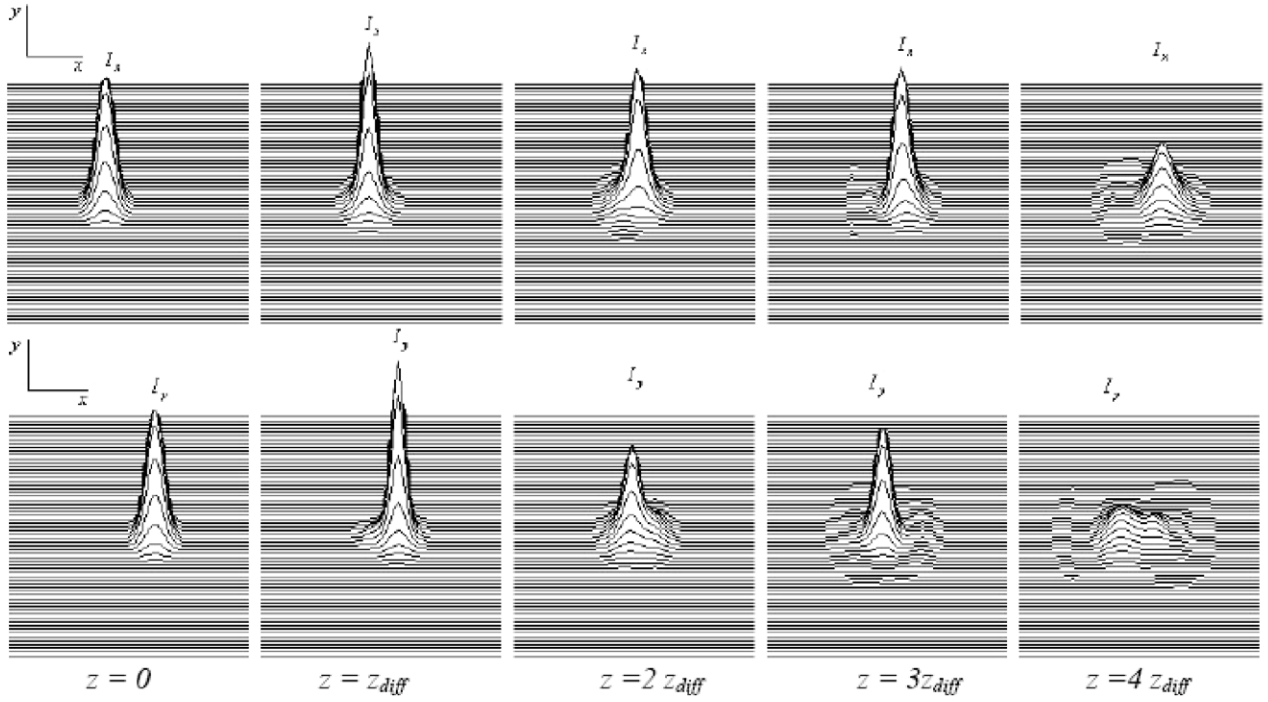

Figure 2. Evolution of the intensity profile I_x of the A_x-component and the intensity profile I_y of the A_y-component of the vector field $\vec{E}$ (presented separately) for the same initial conditions as in figure 1. The periodicity of the energy exchange is observed.

5.1.1. Polarization separated components. The separation of the polarization components can be realized experimentally by means of a system of prisms, where the light pulse falls at the Brewster angle. In this case the initial conditions for numerical solution of the system of equations (7) have the form

$$A_x = A_x^0 \exp\left(-\frac{(x+a)^2 + y^2 + z^2}{2}\right) \exp\,(-\mathrm{i}\Delta v x)$$
$$A_y = A_y^0 \exp\left(-\frac{(x-a)^2 + y^2 + z^2}{2}\right) \exp\,(\mathrm{i}\Delta v x) \exp\left(\mathrm{i}\frac{\pi}{2}\right), \tag{14}$$

where a is the initial shift of the pulses in x-direction with respect to the intersection point and $2\Delta v = 2\, v \sin\theta$ is the normalized relative transverse velocity of the pulses (θ is the angle between the two trajectories).

The crossing of the optical pulses A_x and A_y for $\gamma = 1.8$, $2\Delta v = 0.4$ and $a = 2$ is presented in figure 1. With $I_x = |A_x|^2$ and $I_y = |A_y|^2$ are denoted the intensity profiles of the pulses, while z_{diff} denotes the diffraction lengths $z_{\mathrm{diff}} = k_0 r_0^2$. The (x, y)–(spot) projection of the pulses intensities $I_{x,\,y}(x, y, z = Nz_{\mathrm{diff}}, t = Nz_{\mathrm{diff}}/v_{\mathrm{gr}})$ at distances $z = N^* z_{\mathrm{diff}}$ where $N = 1/2$ is plotted. The behavior of the intensity profiles I_x and I_y separately is shown in figure 2. The intensive periodical energy exchange and simultaneous self-focusing of A_x and A_y is evident. The periodicity of the FFP process can be seen very well in figure 2. In this case the initial energy transfer is from I_x to I_y.

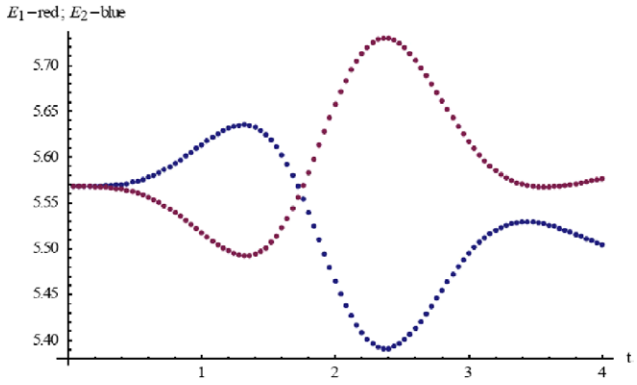

Figure 3. The distribution of the integrals of intensity over time for the both pulses. A periodic energy exchange between laser pulses as function of the time is clearly seen. With E_1 is denoted the integral of intensity of the A_x component and with E_2 the same of the A_y component. The time is normalized on diffraction lengths $t_{\text{diff}} = z_{\text{diff}}/v_{\text{gr}}$. We note the reversal energy flow between the pulses obtained early in the experiment [2]).

Figure 3 shows the distribution of integrals of intensity over time for the both pulses. This is important for the understanding whether the energy transfer between pulses takes place as a result of parametric interaction. We note the same reversal of energy flow between the pulses obtained early in the experiment [2]). In our study the magnitude and direction of energy transfer depend on the initial shift of the pulses a, the relative transverse velocity Δv and the laser intensity γ. Figure 4 presents a similar numerical simulation as figure 1, with $\Delta v = 1$. In this experiment the direction of energy transfer is changed from I_y to I_x. This confirms the experimental results obtained in [3], where similar dependencies of the transfer energy direction on the relative time delay, laser intensities and intersecting angle ($\Delta v = v \sin\theta$) are presented.

5.1.2. Non-separated polarization components. When the laser pulse is split into two arms $\vec{A}_1$ and $\vec{A}_2$ by a regular beam splitter, the obtained filaments contain each of the polarization components. Let $\vec{A}_j = A_{j,x}\vec{x} + A_{j,y}\vec{y}, j = 1, 2$. Then the initial conditions for numerical solution of the system of equations (7) have the form

$$A_x = A_{1,x} + A_{2,x} = \frac{A_1^0}{\sqrt{2}} \exp\left(-\frac{(x+a)^2+y^2+z^2}{2}\right) \exp\left(-\mathrm{i}\Delta v x\right)$$
$$+\frac{A_2^0}{\sqrt{2}} \exp\left(-\frac{(x-a)^2+y^2+z^2}{2}\right) \exp\left(\mathrm{i}\Delta v x\right) \exp\left(\mathrm{i}\frac{\pi}{2}\right)$$
$$A_y = A_{1,y} + A_{2,y}$$
$$= \left\{ \frac{A_1^0}{\sqrt{2}} \exp\left(-\frac{(x+a)^2+y^2+z^2}{2}\right) \exp\left(-\mathrm{i}\Delta v x\right) \right.$$
$$\left. + \frac{A_2^0}{\sqrt{2}} \exp\left(-\frac{(x-a)^2+y^2+z^2}{2}\right) \exp\left(\mathrm{i}\Delta v x\right) \exp\left(\mathrm{i}\frac{\pi}{2}\right) \right\} \exp\left(\mathrm{i}\frac{\pi}{2}\right), \quad (15)$$

where A_x and A_y are composed of the x- and y-components of the two optical pulses propagating along different trajectories.

The interaction of the optical pulses $\vec{A}_1$ and $\vec{A}_2$ for $\gamma = 1.8$, $2\Delta v = 1.6$ and $a = 2$ is shown in figure 5. As in the previous case of separated polarization components we observe the effects of self-focusing and intensive periodical energy exchange. In the faraway zone two additional components in direction orthogonal to the initial pulses are obtained. We suppose that these additional components are connected with the four-wave mixing process. The first prediction and clear experimental observation of additional out-of-plane components was done in [17].

5.2. Energy exchange between two collinear filaments

The propagation through atmosphere of high intensity laser pulse with power two orders of magnitude greater than the critical for self-focusing ($P \sim 100\, P_{\text{cr}}$) leads to breakup of the pulse into many components, each with power around P_{cr} [4]. The basic idea is that filamentation occurs as a consequence of initially present laser wavefront irregularities, enhanced by four-wave mixing. As was reported recently [7], the number of filaments is reduced significantly as a function of the distance. We propose a model based on the degenerate FPP process in order to explain this decreasing number of filaments. Let us suppose that two filaments are at a small distance from each other. Therefore there are conditions for pairing and interaction due to degenerate FPP mixing. The formulation of the problem is similar to the last case in the previous subsection. Let us consider two filaments $\vec{A}_1$ and $\vec{A}_2$ with arbitrary polarization. Let us write the vectors through their x- and y-components $\vec{A}_j = A_{j,x}\vec{x} + A_{j,y}\vec{y}, j = 1, 2$. Then the initial conditions for the numerical solution of the system (7) have the form (14), with relative velocity $\Delta v = 0.00001$ (hence $\theta \sim 0$, i.e. the filaments are collinear).

Figure 6 shows the evolution of two filaments and their exchange of energy by degenerate FPP mixing. We use power close to P_{cr}. Therefore the amplified pulse self-focuses and gets enough power to continue its propagation, while the other pulse gives out energy, enters into linear mode and vanishes. In this way the number of filaments can be reduced by nonlinear parametric processes in $\chi^{(3)}$ media.

6. Conclusions

We have developed a model to describe the recent experimental demonstration of energy exchange between two non-collinear filaments in air, with power close to P_{cr} [1–3]. The authors there point out a possible mechanism based on the generation of a plasma grating at the interaction point. It is known though, that at higher incident laser power, where the plasma plays an important role, the exchange efficiency decreases. In air $P = P_{\text{cr}}$ corresponds to intensity of the laser field of the order of $I \sim 10^{12}$ W cm^{-2}, where the plasma density is too small to form plasma grating.

In this paper we propose another mechanism for this phenomenon on the basis of degenerate FPP mixing. Our numerical investigation confirms the experimental results of periodical energy exchange in the region of overlapping of the two pulses. We obtain also the observed in the experiments

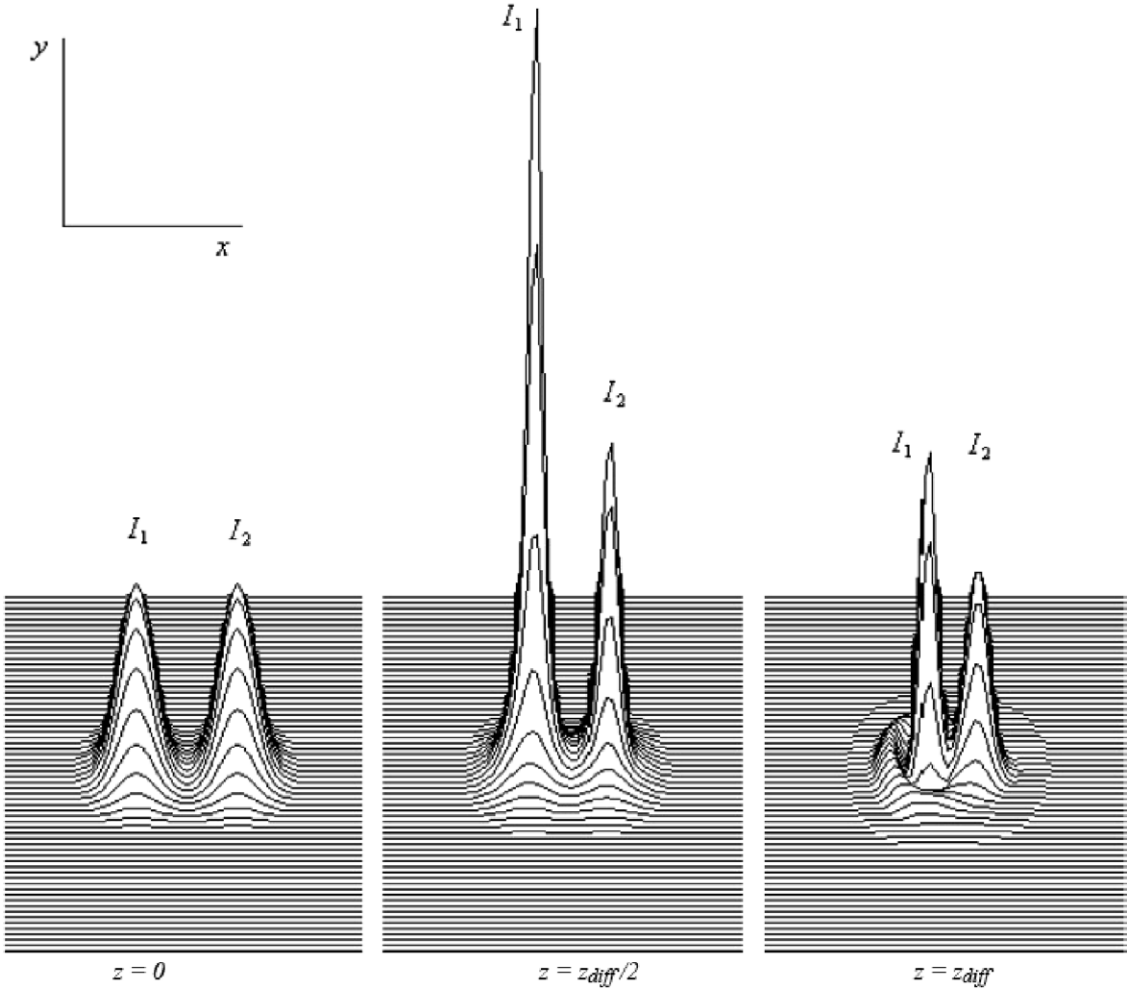

Figure 4. Crossing dynamics between two separated polarization components at initial distance $2a = 4$, transverse velocity difference $2\Delta v = 2$, and nonlinear coefficient $\gamma = 3$, governed by the system of equations (7) with initial conditions (14). The value of the parameter $2\Delta v$ changes the initial phase difference. As a result, the direction of energy transfer is changed from I_y to I_x.

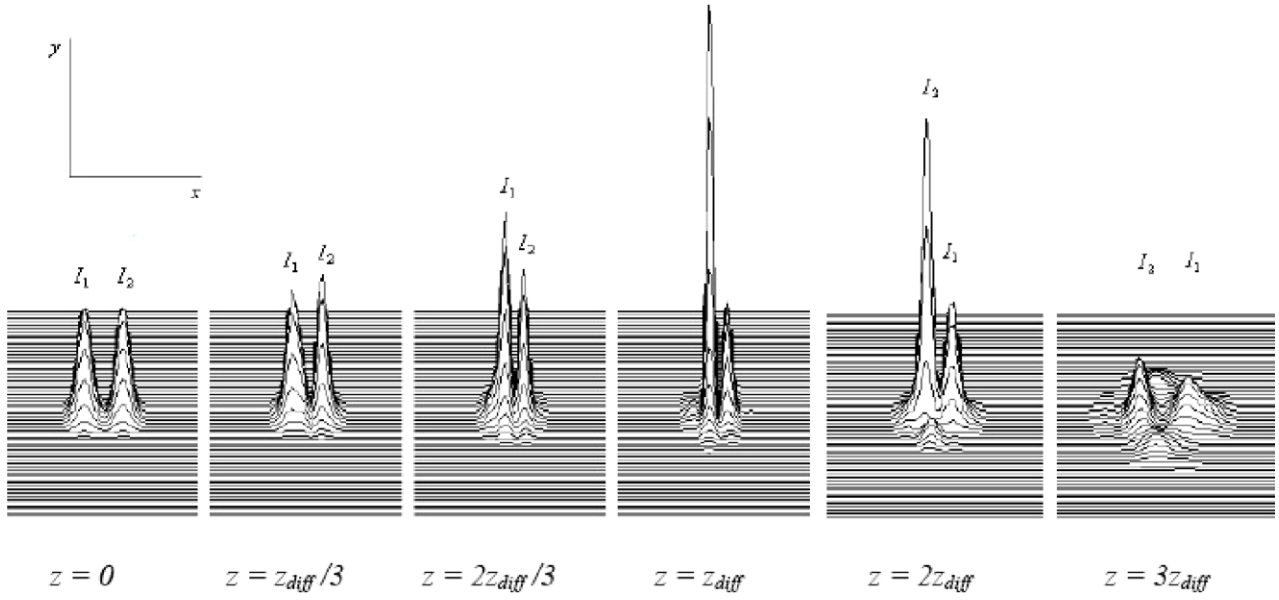

Figure 5. Evolution of two filaments with non-separated polarization components at initial distance $2a = 4$, transverse velocity difference $2\Delta v = 1.6$, and nonlinear coefficient $\gamma = 1.8$, governed by the system of equations (7) with initial conditions (15). We observe self-focusing, periodic exchange of energy and in the faraway zone—generation of two additional components in direction orthogonal to the initial pulses.

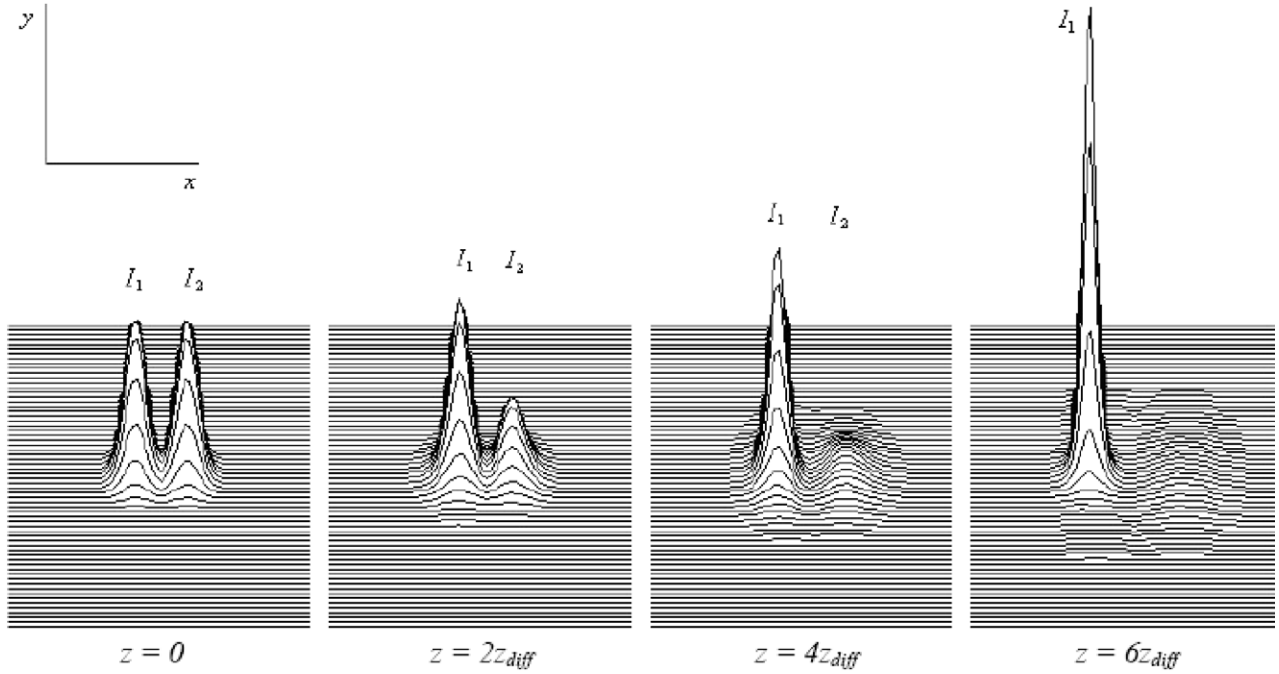

Figure 6. Energy exchange between two collinear filaments $\vec{A}_1$ and $\vec{A}_2$ at small a distance $2a = 3.4$ governed by the system of equations (7) with initial conditions (15) at values of the parameters $v = 0.00001$ and $\gamma = 3$. Due to degenerated FPP mixing one of the filaments is amplified while the other filament enters in linear mode and vanishes.

dependence of the initial energy transfer on the relative transverse velocity (crossing angle), intensity and initial phase difference (distance a). When the pulse A_1 has positive initial phase with respect to pulse A_2 (depending on the above parameters), initially pulse A_1 takes energy from pulse A_2 and vice versa. As pointed out in [4], the degenerate FPP processes play an important role in the multi-filament generation. Another important effect, which was observed experimentally in the multi-filament propagation, is that the number of filaments N with power arround P_{cr} decreases gradually with propagation distance [5–7]. The authors explain this with energy losses by plasma or multi-photon absorbtion. We think, though, that for intensities of the order of $I \sim 10^{12}$ W cm^{-2} the multi-photon processes and plasma are very weak to play such an important role in this process. That is why we turn back to the theory developed by Boyd [4], and we extend it now to evolution equations for pairing of pulses by degenerate FPP process. The result is that one of the pulses is amplified, while the other one decreases in energy, enters in linear mode and vanishes. Thus, the degenerate FPP process is a natural explanation of the reducing of the number of filaments with power around P_{cr}. Another important result in this study is that we investigate the filament and the filament's interaction as a vector field. Beyond the scope of the specific task, we have shown that the vector representation of the problems removes the disadvantages of the use of the generalized nonlinear polarization operator (2), making it a useful tool in the solution of different problems, connected with third-order polarization. We plan to use in the future this (or a similar) vector system for description of the observed in [18] FPP vector solitons.

Acknowledgments

This work was supported in part by Bulgarian Science Fund under grant DFNI I-02/9.

References

[1] Bernstein A C, Mc Cormick M, Dyer G M, Sanders J C and Ditmire T 2009 *Phys. Rev. Lett.* **102** 123902
[2] Liu Y, Durand M, Chen S, Houard A, Prade B, Forestier B and Mysyrowicz A 2010 *Phys. Rev. Lett.* **105** 055003
[3] Pengji D *et al* 2013 *Opt. Express* **21** 27631–41
[4] Boyd R W 2003 *Nonlinear Optics* (New York: Academic)
[5] Chin S L *et al* 2005 *Can. J. Phys.* **83** 863–905
[6] Couairon A and Mysyrowicz A 2007 *Phys. Rep.* **441** 47–189
[7] Magali D *et al* 2013 *Opt. Express* **21** 26836
[8] Braun A, Korn G, Liu X, Du D, Squier J and Mourou G 1995 *Opt. Lett.* **20** 73–5
[9] Maker P D and Terhune R W 1965 *Phys. Rev.* **137** A801
[10] Kolesik M and Moloney J V 2008 *Opt. Express* **16** 2971
[11] Kolesik M, Wright E M, Becker A and Moloney J V 2006 *Appl. Phys.* B **85** 531–8
[12] Kovachev L M 2009 *J. Mod. Opt.* **56** 1797–803
[13] Borodin A V *et al* 2013 *Opt. Lett.* **38** 1906–9
[14] Kovachev L and Kovachev K 2011 *Laser Systems for Applications* (Rijeka: InTech) part 3, chapter 11
[15] Sheinfux A H, Schleifer E, Papeer J, Gibich G, Ilan B and Zigler A 2012 *Appl. Phys. Lett.* **101** 201105
[16] Agrawal G P 2007 *Nonlinear Fiber Optics* 4th edn (New York: Academic)
[17] Dergachev A A, Kadan A A and Shlenov S A 2012 *Quantum Electron.* **42** 125–30
[18] Wang R *et al* 2012 *Opt. Express* **20** 14168